Nanoscale

PAPER

Polyaniline:poly(sodium 4-styrenesulfonate)-stabilized gold nanoparticles as efficient, versatile catalysts†

Cite this: *Nanoscale*, 2014, **6**, 5223

Xiaojun Liu,[a] Ligui Li,*[a] Meixia Ye,[a] Yang Xue[a] and Shaowei Chen*[ab]

Gold nanoparticles were stabilized by a polyaniline:poly(sodium 4-styrenesulfonate) (PANI:PSS) matrix and readily dispersed in water over a wide range of pH. In contrast to nanoparticles passivated by alkanethiolates that formed a compact capping layer on the nanoparticle surface, the PANI:PSS–Au nanocomposites exhibited apparent catalytic activity in the reduction of 4-nitrophenol in the presence of excessive $NaBH_4$, with reasonably good recyclability, which was likely due to the large accessible surface area. In addition, the PANI:PSS–Au nanocomposites also demonstrated peroxidase-like catalytic activity as evidenced by the colorimetric detection of H_2O_2 and glucose with PANI:PSS–Au as the enzymatic mimic. The present method may find potential applications in the design, preparation and functionalization of noble nanoparticles as efficient, versatile, and recyclable catalysts with high dispersibility and stability in aqueous media.

Received 17th January 2014
Accepted 14th February 2014

DOI: 10.1039/c4nr00328d

www.rsc.org/nanoscale

1. Introduction

Gold nanoparticles have attracted considerable attention due to their various inherent advantages such as the ease of synthesis, high chemical stability and size-dependent optical, electronic, and catalytic properties, which lead to diverse applications including chemical/biological sensing, surface-enhanced Raman scattering, (nano)electronics, catalysis, and so on.[1–6] Yet, without a suitable support, gold nanoparticles can easily aggregate in solution, which results in substantial reduction of their catalytic activities. An effective way to prevent aggregation of the nanoparticles is to utilize appropriate stabilizers. So far, thiolate derivatives have been used extensively as the ligands of choice to stabilize metal nanoparticles, forming a (metal)core–(organic)shell structure, by taking advantage of the strong affinity of thiols to metal surfaces.[6–11] The thus-obtained nanoparticles exhibit excellent dispersibility and stability in solutions. However, it has been shown that the presence of a densely packed capping layer on the metal nanoparticle surface may compromise the catalytic activity as the surface active sites become inaccessible and the compact capping layer introduces steric hindrance for the inward diffusion of reactants to Au cores and the outward diffusion of reaction products.[12–16] Moreover, the insulating thiolate ligand layers may impede electronic interactions between the nanoparticles and the supporting substrates, rendering it difficult to exploit the synergetic effect of these two components as compared to those in direct contact.[17–19]

Within this context, in catalytic applications metal nanoparticles are typically supported on substrate surfaces where no organic capping ligands are used and hence the surface is presumably readily accessible.[20,21] Yet as the corresponding catalysts are not dispersible in the reaction media and the reactions are heterogeneous in nature, the catalytic activity may be compromised, as compared to homogeneous catalysis. Therefore, one question arises: is it possible to prepare metal nanocatalysts where the nanoparticles are readily dispersed into the reaction media and yet exhibit a large accessible surface area? This is the primary motivation of the present work. To the best of our knowledge, there are relatively few reports on the preparation of highly dispersible and stable Au nanoparticles with a largely accessible surface.[22,23]

Polyaniline is one of the most frequently used supports for metal nanoparticles not only because it can directly reduce metal cations to produce nanoparticles, but also because of its diverse advantages such as completely reversible doping/dedoping chemistry, high environmental stability, simple synthesis under mild conditions and low cost.[24–30] Furthermore, when PANI is doped by acid to form emeraldine salt (Scheme S1†), the nanostructures of PANI become hydrophilic, and hence render the PANI-supported metal nanoparticles readily dispersible in aqueous solutions. However, metal nanoparticles supported by PANI alone are not stable, forming

[a]*New Energy Research Institute, School of Environment and Energy, South China University of Technology, University Town, Guangzhou 510006, China. E-mail: esguili@scut.edu.cn; shaowei@ucsc.edu*

[b]*Department of Chemistry and Biochemistry, University of California, 1156 High Street, Santa Cruz, California 95064, USA*

† Electronic supplementary information (ESI) available: Structural scheme, HRTEM micrograph, UV-vis absorption spectra and photographs. See DOI: 10.1039/c4nr00328d

aggregates in solution even after standing for only a few minutes. In addition, the dispersibility of PANI-supported metal nanoparticles will quickly diminish when they are used as catalysts in alkaline solutions due to the formation of a hydrophobic emeraldine base resulting from dedoping.[31] These disadvantages restrict the applications of PANI-supported metals nanoparticles in catalysis.

In the present work, we use highly stable PANI:PSS colloids[32] as support and reducing agents to prepare Au nanoparticles. Unlike Au nanoparticles capped by PANI alone, the resulting nanocomposites exhibit excellent dispersibility and stability in water in a wide range of pH. Importantly, the thus-obtained nanocomposites demonstrate apparent catalytic activity in various reactions, as highlighted by the reduction of 4-nitrophenol into 4-aminophenol, as compared to the conventionally thiolate-protected counterparts; and the catalysts may be easily recovered by dialysis and reused. Furthermore, the PANI:PSS–Au nanocomposites may act as peroxidase mimics and exhibit peroxidase-like catalytic activity in the catalytic oxidation of 3,3′,5,5′-tetramethylbenzidine (TMB) by H_2O_2.[8,33,34] Such unique characteristics can then be exploited for the specific detection of glucose by simple colorimetric analysis of the reaction dynamics. The present method may find potential applications in the design and preparation of noble metal nanoparticles as efficient, versatile, and recyclable catalysts with high dispersibility and stability in aqueous solutions.

2. Experimental section

2.1 Materials

Aniline (anhydrous, 98%) and ammonium peroxydisulfate (98%) were purchased from Alfa Aesar Company. Aniline was distilled under reduced pressure before use. PSS (MW 70 000) was purchased from Sigma Aldrich. 4-Nitrophenol, acetic acid, sodium hydroxide, 3,3′,5,5′-tetramethylbenzidine (TMB), glucose, fructose, lactose, maltose, glucose oxidase (GOD) (>180 U mg^{-1}) and tetrachloroauric acid were purchased from Aladdin Reagents Inc. Water was supplied using a Barnstead Nanopure Water System (18.3 mΩ cm).

2.2 Sample preparation

2.2.1 Preparation of PANI:PSS colloids and PANI nanofibers. Highly stable PANI:PSS colloids were prepared by using the method reported previously.[32] In brief, a calculated amount of aniline was dissolved in an aqueous solution of acetic acid (0.2 M) at a final concentration of 32 mM. PSS was dissolved in an aqueous solution of 8 mM ammonium peroxydisulfate and 0.2 M acetic acid. The aniline and PSS solutions were then mixed in a beaker under vigorous stirring for 5 min while polymerization occurred. The mixture was then placed in the dark for 24 h at room temperature until the polymerization reaction was complete. The molar ratio of aniline and the 4-styrenesulfonate repeating unit in PSS was 2 : 1 unless otherwise indicated. Excessive acid and unreacted molecules were removed from the PANI:PSS dispersions by means of dialysis (dialysis tube, 2000 g mol^{-1} cut-off) in Nanopure water.

PANI nanofibers were prepared in a similar way but without the addition of PSS.[31]

2.2.2 Functionalization of gold nanoparticles on PANI. To prepare Au nanoparticles on PANI nanofibers (denoted as PANI–Au) or PANI:PSS colloids (denoted as PANI:PSS–Au), a calculated amount of 0.0482 M tetrachloroauric acid solution was added into the PANI or PANI:PSS dispersion drop by drop under magnetic stirring. The mixture was continuously stirred for 24 h and then dialyzed in Nanopure water to remove unreacted Au(III) precursors.

The gold content in the composites was quantitatively determined by using inductively coupled plasma atomic emission spectrometric (ICP-AES) measurements. The results showed that the gold concentration in the above-obtained PANI–Au and PANI:PSS–Au dispersions was 85.04 and 89.44 mg L^{-1}, respectively, which indicated that 86.3% and 90.8% of the corresponding Au(III) precursors were reduced to Au nanoparticles. This also shows that the gold content in both composites is highly comparable.

To prepare thiolate-capped PANI:PSS–Au nanocomposites, mercaptoacetic acid was added into the PANI:PSS–Au dispersion prepared above at a final concentration of 10 mM. The mixed solution was kept in the dark overnight and then transferred to a dialysis tube (2000 g mol^{-1} cut-off) to remove excess mercaptoacetic acid. The final product is denoted as PANI:PSS/MAA–Au.

2.3 Characterization

2.3.1 Instrumentation. Transmission electron microscopic (TEM) measurements were conducted using a JEOL JEM-1011 transmission electron microscope operating at an acceleration voltage of 100 kV. Wide-angle X-ray diffraction (WAXD) profiles were obtained by using a Bruker D8 Discover XRD system operating at 40 kV and 40 mA. The diffraction patterns were recorded in a θ–2θ symmetry scanning mode within the range of 30° to 90°. UV-vis absorption spectra were acquired with a UV 2300 spectrometer (Shanghai Techcomp Bio-Equipment Ltd).

2.3.2 Reduction of 4-nitrophenol catalyzed by gold nanoparticles. In a typical experiment, 300 μL of the PANI:PSS–Au solution (5.0×10^{-5} M in water), 850 μL of 4-nitrophenol (0.2 mM aqueous solution) and 500 μL of freshly prepared $NaBH_4$ (25 mM aqueous solution) were mixed in a 5 mL glass vial. The mixed solution was then quickly transferred to a cuvette for UV-vis absorption measurements. Nanopure water was used as the reference. All the experiments were carried out at room temperature. To evaluate the reusability of the catalysts, the catalysts were recovered by dialysis in water for 4 h and then used for a new round of tests.

Reactions with PANI–Au and PANI:PSS/MAA–Au were carried out in a similar fashion at the same effective gold concentration.

2.3.3 TMB–H_2O_2 reactions catalyzed by gold nanoparticles. The TMB–H_2O_2 reactions were monitored by colorimetric detection of H_2O_2. Experimentally, 50 μL of a freshly prepared TMB solution (20 mM in ethanol), 50 μL of PANI:PSS–Au nanocomposites (5.0×10^{-5} M in water), 50 μL of H_2O_2 at

different concentrations and 350 μL of an acetate buffer (0.5 M, pH = 4.1) were mixed in a glass vial. The mixed solution was incubated in a water bath set at 45 °C for 30 min, and then transferred to a cuvette for UV-vis absorption measurements.

Reactions with PANI–Au and PANI:PSS/MAA–Au were carried out in a similar fashion at the same effective gold concentration.

2.3.4 Glucose detection using gold nanoparticles and glucose oxidase. The colorimetric detection of glucose was carried out by using a modified method reported previously.[8] The procedure includes four steps: (1) 50 μL of 5.0 mg mL^{-1} GOD and 200 μL of glucose at various concentrations in a 10 mM phosphate buffer solution (pH = 7.3) were incubated in a water bath set at 37 °C for 30 min; (2) into this solution were then added 50 μL of TMB (20 mM in ethanol), 50 μL of PANI:PSS–Au nanocomposites (5.0×10^{-5} M in Nanopure water) and 350 μL of an acetate buffer (0.5 M, pH = 4.1); (3) the resulting solution was incubated in a water bath at 45 °C for 30 min; and (4) finally, the solution was transferred to a cuvette for UV-vis absorption measurements.

To check the specificity of the PANI:PSS–Au nanocomposites to glucose, measurements were also carried out by using other sugars such as fructose, maltose and lactose at a concentration of 5.0 mM in place of glucose.

3. Results and discussion

As shown in Fig. 1a, gold nanoparticles may be readily synthesized by using acetic acid-doped PANI:PSS colloids as both the supporting substrates and reducing agents. It can be seen that gold nanoparticles (dark contrast objects) were well separated on a low-contrast background which was the PANI:PSS matrix, indicative of effective protection of the nanoparticles by PANI:PSS against aggregation. Statistical analysis based on over two hundred nanoparticles shows that the majority of the gold nanoparticles are *ca.* 10.0 ± 0.7 nm in diameter, as manifested by the core size histogram in Fig. 1b. Furthermore, from the high-resolution TEM image in Fig. 1c, one can see clearly defined lattice fringes with a spacing of 0.24 nm (Fig. S1†), which are consistent with the (111) crystallographic planes of face-centered cubic (fcc) gold, indicating the highly crystalline nature of the gold nanoparticles.

Fig. 1d shows the XRD studies of the PANI:PSS–Au composite where one can see five rather apparent diffraction peaks at 38.22°, 44.46°, 64.77°, 77.71°, and 81.80°, which can be indexed to the (111), (200), (220), (311), and (222) planes of fcc gold crystallites, respectively. The size of the crystallites along the [111] direction was estimated to be 9.9 ± 0.5 nm based on the calculation using the Scherrer equation, in good agreement with the TEM result in Fig. 1b. In contrast, with PANI alone (Fig. 1e), whereas gold nanoparticles could also be produced, the nanoparticles were about 10 times larger with an average diameter around 100.0 ± 3.2 nm, as depicted in the core size histogram in Fig. 1f.

The discrepancy of the size of the gold nanoparticles produced in the presence of PANI:PSS and PANI alone may be ascribed to the difference of "effective aniline" concentration in the synthetic process. Generally, only the aniline repeating units on the surface of the PANI nanostructures are accessible to Au(III) and effective in the redox reactions. In the PANI:PSS colloids (Fig. 1a) which were only several nanometers in size as determined by dynamic light scattering measurements,[32] a large number of aniline repeating units were on the surface and might be readily accessible to Au(III) precursors leading to the

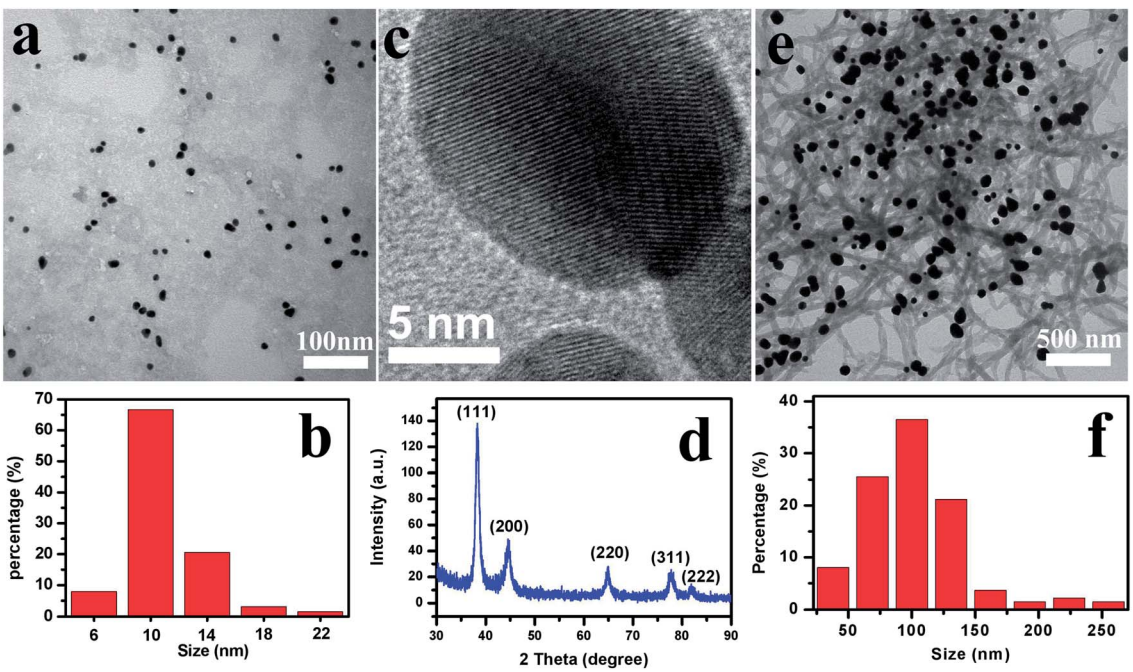

Fig. 1 (a and c) TEM micrographs, (b) core size histogram and (d) XRD patterns of the PANI:PSS–Au nanocomposites. Panels (b) and (f) are the TEM micrograph and core size histogram of the PANI:Au counterparts, respectively.

production of relatively small gold nanoparticles. In contrast, for the PANI nanofibers in Fig. 1b, the dimensions were much larger (*ca.* 50 nm in width and 1 μm in length), and the surface area was about one order of magnitude smaller than that of the PANI:PSS colloids. That is, the number of accessible aniline units decreased accordingly. As a result, much larger gold nanoparticles were formed on the PANI nanofiber surface.

Interestingly, the PANI:PSS–Au nanocomposites could be readily dispersed in water and remained stable in a wide range of pH from 1 to 12 (Fig. S2†). In contrast, the PANI–Au nanocomposites gradually precipitated from water regardless of the solution pH.

The catalytic activity of the nanocomposites prepared above was then investigated and compared by using the reduction of 4-nitrophenol into 4-aminophenol in the presence of excessive $NaBH_4$ as an illustrating example. This reaction has been used extensively as a benchmark to quantify the catalytic activity of various metallic nanoparticles,[20,35,36] as the reaction dynamics can be easily monitored by UV-vis absorption spectroscopy. Experimentally, upon the addition of excessive $NaBH_4$ into a 4-nitrophenol solution, the color of the solution quickly changed from light yellow to green yellow. Fig. 2a depicts the UV-vis absorption spectra of a 4-nitrophenol solution in the presence of PANI:PSS–Au nanocomposites collected at different reaction intervals. At the beginning of the reaction (0 s, black curve), the solution exhibited a major absorption peak at 400 nm and a small one at 318 nm. This is due to the formation of 4-nitrophenolate anions under basic conditions. The intensity of the peak at 400 nm decreased quickly with time, and concurrently the intensity of the peak at 300 nm increased. The reaction appeared to complete within 140 s. Note that the absorption peak at 300 nm is characteristic of 4-aminophenol.[35,37,38] The results in Fig. 2a clearly indicate effective reduction of 4-nitrophenol into 4-aminophenol in the presence of PANI:PSS–Au.

Since the reaction was conducted under a large excess of $NaBH_4$, the reaction rate was nearly independent of the $NaBH_4$ concentration, and consequently the kinetics can be modeled by a quasi-first-order process with regard to the concentration of 4-nitrophenol. Fig. 2b depicts the plot of $\ln(A_t/A_0)$ as a function of reaction time (t), where A_t and A_0 are the absorption intensities at 400 nm at time t and 0, respectively. A kinetic rate constant (k) of 2.17×10^{-2} s^{-1} can be derived from linear regression of the experimental data (blue squares). Reactions with PANI–Au and PANI:PSS/MAA–Au were carried out in a similar fashion (Fig. S3a and b†), and the dynamic plots are also included in Fig. 2b. It can be seen that whereas PANI–Au also exhibited apparent catalytic activity, the rate constant (k) was markedly lower by one order of magnitude at 2.10×10^{-3} s^{-1} (red diamonds). In the experimental measurements with mercaptoacetic acid-functionalized PANI:PSS/MAA–Au nanocomposites (black circles) which were prepared to mimic the traditional thiolate-capped gold nanoparticles, the catalytic activity was significantly impeded with an induction period of about 300 s where no apparent reaction occurred with a drastically reduced rate constant of 5.23×10^{-3} s^{-1} at longer reaction times. This may be ascribed to the steric hindrance of the densely packed thiolate layers on the Au nanoparticle surface.

An additional control experiment was carried out by adding only $NaBH_4$ to 4-nitrophenol but without gold nanoparticles. The UV-vis absorption profiles remained unchanged for up to 45 min, indicating that no reduction of 4-nitrophenol into 4-aminophenol occurred in the absence of gold nanoparticle catalysts (Fig. S3c†).

For noble metal-based catalysts, reusability is also desired for practical applications. Thus, to check the reusability of the above PANI:PSS supported gold nanoparticle catalysts, we collected and purified the nanocomposites by dialysis and measured their catalytic activity in repeat tests of the reduction of 4-nitrophenol under the otherwise identical experimental conditions. Fig. 2c depicts the reaction dynamics in five cycles of catalytic reactions, from which the kinetic rate constants (k) were evaluated by linear regression and summarized in Table 1. It can be seen that the catalytic activity remained rather apparent; yet the rate constant did show a gradual decrease with repeat cycles, from 2.17×10^{-2} s^{-1} at the first cycle to

Table 1 Kinetic rate constant (k) in different repeat cycles of the catalytic reduction of 4-nitrophenol by PANI:PSS–Au in the presence of excessive $NaBH_4$

Use time	1st	2nd	3rd	4th	5th
k ($\times 10^{-2}$ s^{-1})	2.17	1.85	1.21	0.72	0.54

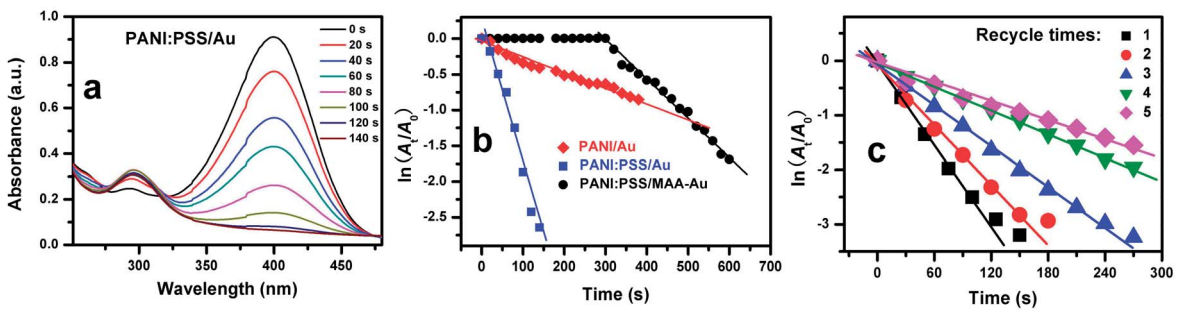

Fig. 2 (a) Time-dependent UV-vis absorption spectra of the reduction of 4-nitrophenol by $NaBH_4$ in the presence of PANI:PSS–Au. (b) Plot of $\ln(A_t/A_0)$ as a function of time for the reaction catalyzed by PANI–Au, PANI:PSS–Au and PANI:PSS/MAA–Au. (c) Plot of $\ln(A_t/A_0)$ as a function of time for the reaction catalyzed by PANI:PSS–Au at different repeat cycles.

0.54×10^{-2} s^{-1} at the fifth. This may be due to the dilution effect and loss of catalysts during the dialysis process.

Interestingly, in acidic solutions, the PANI:PSS–Au nanocomposites also demonstrated peroxidase-like catalytic activity, as exemplified by the apparent oxidation of TMA by H_2O_2 (Scheme 1). This can be clearly seen in the inset of Fig. 3a, where upon the addition of PANI:PSS–Au nanoparticles, the TMB–H_2O_2 solution exhibited a marked color change from greenish yellow to blue. This is because the oxidation product, 3,3′,5,5′-tetramethylbenzidine diimine, exhibits a distinct blue color with an absorption band centered at *ca.* 650 nm. In sharp contrast, the addition of PANI–Au did not lead to an apparent change of the solution color, as compared to that of the blank solution containing only TMB and H_2O_2, indicating minimal activity of PANI–Au in the oxidation of TMB by H_2O_2. No catalytic activity was observed with the PANI:PSS/MAA–Au nanocomposites, either. Note that H_2O_2 may be activated by peroxidases and participate in numerous oxidations in biological systems and hence accurate determination of H_2O_2 is important in many fields such as pharmacy, clinic diagnostics, the food industry, and environmental safety.[39,40] The above observations show that the PANI:PSS–Au nanocomposites may serve as effective peroxidase mimics with apparent advantages over the natural counterparts such as the ability to work in harsh environments, easy preparation, purification and storage, and low cost.

The superior catalytic activity of PANI:PSS–Au can be quantified in UV-vis absorption measurements. As shown in Fig. 3a, in contrast to the blank solution (black curve), the solution with PANI:PSS–Au shows two rather strong absorption peaks at 654 nm and 900 nm after incubation of the solution at 45 °C for 30 min (red curve). These are consistent with the formation of chromophores as the oxidation products of TMB by H_2O_2.[8,41,42] Yet, virtually no absorption features can be identified in the presence of PANI–Au (blue curve) or PANI:PSS/MAA–Au (green curve), indicative of little catalytic activity of these two composites. Fig. 3b depicts the variation of the solution absorbance at 654 nm with H_2O_2 concentration (corresponding spectra in Fig. S4†), which exhibits a linear correlation within the range of 3.3 to 330 μM with an estimated detection limit of 2.0 μM. In other words, the PANI:PSS–Au nanocomposites may be used for quantitative determination of H_2O_2 down to the micromolar concentration range.

It has been shown that when H_2O_2 is adsorbed on Au nanoparticle surfaces, the O–O bond will break to form double HO˙ radicals.[8,43] Subsequently, the generated radicals may be stabilized by partial charge transfer to the conduction band of Au nanoparticles,[44,45] and involved in the oxidation of TMB. Thus, the apparent catalytic activity of PANI:PSS–Au nanocomposites in TMB oxidation by H_2O_2 may again be ascribed to the ready accessibility of the gold surface as well as the negatively charged PSS layer that enhanced the adsorption of TMB onto the particle surface. In contrast, for the PANI–Au nanocomposites, the lack of stable dispersion in the water solution and the positively charged PANI layer did not favor the uptake of TMB; and for PANI:PSS/MAA–Au, the mercapto surface passivation layer constituted a significant steric hindrance for the adsorption of both H_2O_2 and TMB onto the Au surface, resulting in minimal catalytic activity.[8]

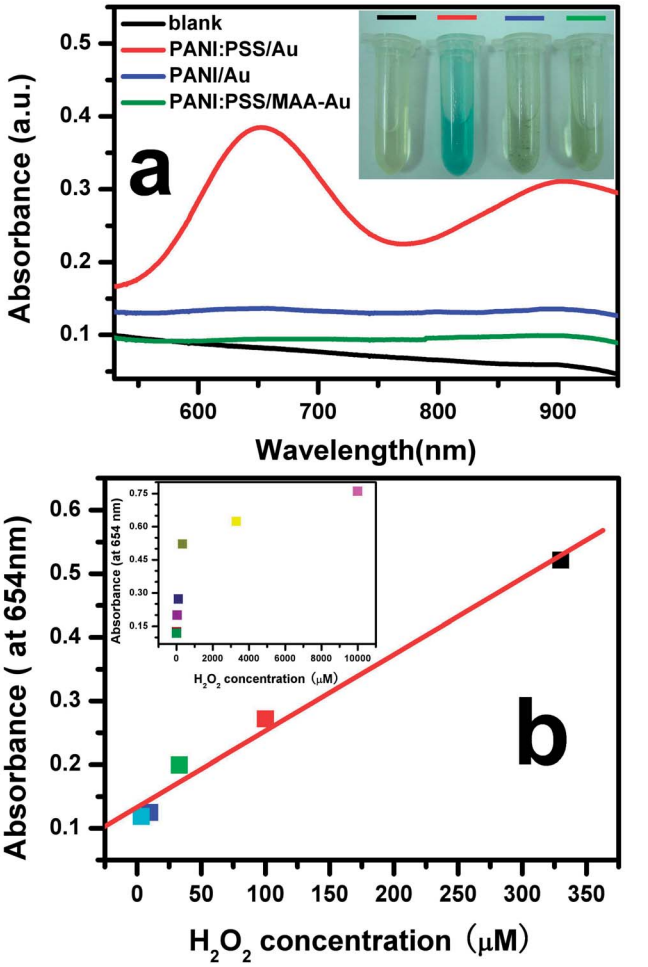

Fig. 3 (a) UV-vis absorption spectra of a TMB–H_2O_2 solution in the absence (blank, black curve) and presence of PANI:PSS–Au (red curve), PANI–Au (blue curve), and PANI:PSS/MAA–Au (green curve), respectively. All the solutions were incubated at 45 °C for 30 min. The inset shows the color of corresponding solutions after incubation. (b) Linear calibration plot between the absorbance intensity at 654 nm and H_2O_2 concentration (up to 330 μM). The inset shows the absorbance intensity at 654 nm as a function of H_2O_2 concentration in the range of 3.3 to 10 000 μM.

Such a unique property may be exploited for the specific detection of glucose by colorimetric analysis, in combination with GOD, which has long been known to catalyze the oxidation of glucose into H_2O_2 and D-glucono-δ-lactone.[46] Experimentally, it was observed when glucose at various concentrations was added into a solution containing a calculated amount of

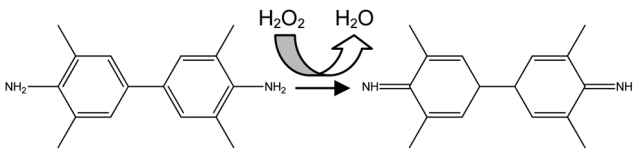

Scheme 1

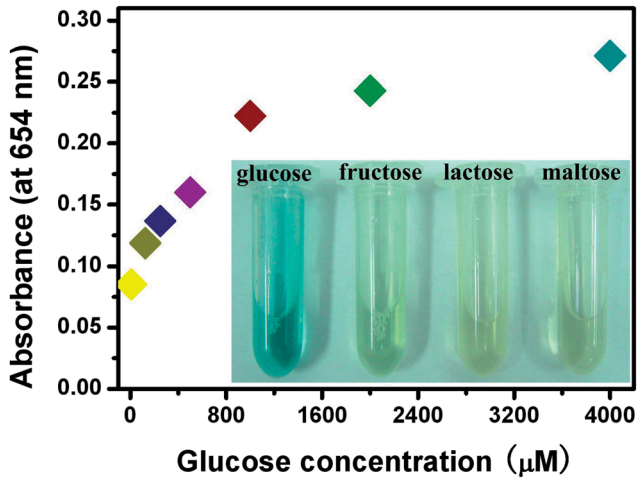

Fig. 4 Absorption intensity at 654 nm at various concentrations of glucose. The inset shows the color of the corresponding solutions after incubation.

PANI:PSS–Au nanocomposites, GOD and TMB in a phosphate buffer solution (Fig. S5†), the solution exhibited an apparent color change to blue, signifying the oxidation of TMB (Scheme 1) by H_2O_2 produced from the oxidation of glucose catalyzed by GOD. Fig. 4 depicts the variation of the absorbance at 654 nm with glucose concentration. One can see a linear correlation in the concentration range of 8.0 to 1000 μM, with an estimated detection limit of 4.0 μM. This response is highly specific to glucose. As shown in the figure inset, the solution color changed to blue only with the addition of glucose, but remained virtually unchanged in the presence of fructose, lactose, and maltose even at a concentration as high as 5.0 mM.

Taken together, the observations described above explicitly demonstrate that the PANI:PSS–Au nanocomposites displayed superior catalytic activity over PANI–Au and PANI:PSS/MAA–Au in various homogeneous catalytic reactions. Future work will focus on optimization of the synthetic conditions such as temperature, the concentration of reactants and reaction time to further reduce the size of the Au nanoparticles and to maximize the catalytic activity of the PANI:PSS–Au nanocomposites.

4. Conclusions

In summary, ultrafine PANI:PSS colloids were used as both reductants and stabilizers to prepare PANI:PSS–Au nanocomposites that were highly dispersible and stable in water in a wide range of pH. The materials were found to exhibit apparent catalytic activity and good reusability in various homogeneous reactions, in contrast to PANI–Au or PANI:PSS/MAA–Au nanocomposites. This was ascribed to a large interface between Au nanoparticles and aniline repeating units and ready accessibility of the gold surface. Significantly, the PANI:PSS–Au nanocomposites demonstrated peroxidase-like catalytic activity, which might be exploited for the colorimetric detection of H_2O_2. Furthermore, it can be used as an effective peroxidase mimic to quantitatively determine glucose concentration. The results show that deliberate surface functionalization is important in the design and preparation of noble metal nanoparticles as efficient, versatile and recyclable catalysts with high dispersibility and stability in aqueous media.

Acknowledgements

This work was supported by the National Recruitment Program of Global Experts. L.G.L acknowledges financial support from the Fundamental Research Funds for the Central Universities (Grant no. 2013ZM0019).

Notes and references

1 R. G. Chaudhuri and S. Paria, *Chem. Rev.*, 2012, **112**, 2373.
2 D. Wang and Y. Li, *Adv. Mater.*, 2011, **23**, 1044.
3 K. Saha, S. S. Agasti, C. Kim, X. Li and V. M. Rotello, *Chem. Rev.*, 2012, **112**, 2739.
4 L. Dykman and N. Khlebtsov, *Chem. Soc. Rev.*, 2012, **41**, 2256.
5 E. C. Dreaden, A. M. Alkilany, X. Huang, C. J. Murphy and M. A. El-Sayed, *Chem. Soc. Rev.*, 2012, **41**, 2740.
6 M.-C. Daniel and D. Astruc, *Chem. Rev.*, 2004, **104**, 293.
7 J. Shan and H. Tenhu, *Chem. Commun.*, 2007, 4580.
8 Y. Jv, B. Li and R. Cao, *Chem. Commun.*, 2010, **46**, 8017.
9 L. Shang, N. Azadfar, F. Stockmar, W. Send, V. Trouillet, M. Bruns, D. Gerthsen and G. U. Nienhaus, *Small*, 2011, **7**, 2614.
10 R. Jin, *Nanoscale*, 2010, **2**, 343.
11 R. Sardar, A. M. Funston, P. Mulvaney and R. W. Murray, *Langmuir*, 2009, **25**, 13840.
12 R. M. Crooks, M. Zhao, L. Sun, V. Chechik and L. K. Yeung, *Acc. Chem. Res.*, 2001, **34**, 181.
13 Y. Lu, Y. Mei, M. Drechsler and M. Ballauff, *Angew. Chem., Int. Ed.*, 2006, **45**, 813.
14 M. M. Nigra, J.-M. Ha and A. Katz, *Catal. Sci. Technol.*, 2013, **3**, 2976.
15 W. Liu, X. Yang and L. Xie, *J. Colloid Interface Sci.*, 2007, **313**, 494.
16 J. A. Lopez-Sanchez, N. Dimitratos, C. Hammond, G. L. Brett, L. Kesavan, S. White, P. Miedziak, R. Tiruvalam, R. L. Jenkins, A. F. Carley, D. Knight, C. J. Kiely and G. J. Hutchings, *Nat. Chem.*, 2011, **3**, 551.
17 S. Chen, Z. Wei, X. Qi, L. Dong, Y.-G. Guo, L. Wan, Z. Shao and L. Li, *J. Am. Chem. Soc.*, 2012, **134**, 13252.
18 H. Xu, L.-X. Ding, C.-L. Liang, Y.-X. Tong and G.-R. Li, *NPG Asia Mater.*, 2013, **5**, e69.
19 X. Zhang and Z. Su, *Adv. Mater.*, 2012, **24**, 4574.
20 H.-L. Jiang, T. Akita, T. Ishida, M. Haruta and Q. Xu, *J. Am. Chem. Soc.*, 2011, **133**, 130.
21 D. Matthey, J. G. Wang, S. Wendt, J. Matthiesen, R. Schaub, E. Lægsgaard, B. Hammer and F. Besenbacher, *Science*, 2007, **315**, 1692.
22 X. Wang, Y. Long, Q. Wang, H. Zhang, X. Huang, R. Zhu, P. Teng, L. Liang and H. Zheng, *Carbon*, 2013, **64**, 499.
23 K. L. McGilvray, M. R. Decan, D. Wang and J. C. Scaiano, *J. Am. Chem. Soc.*, 2006, **128**, 15980.

24 H. D. Tran, J. M. D'Arcy, Y. Wang, P. J. Beltramo, V. A. Strong and R. B. Kaner, *J. Mater. Chem.*, 2011, **21**, 3534.
25 J. Huang and R. B. Kaner, *J. Am. Chem. Soc.*, 2004, **126**, 851.
26 J. Han, L. Li and R. Guo, *Macromolecules*, 2010, **43**, 10636.
27 D. Li, J. Huang and R. B. Kaner, *Acc. Chem. Res.*, 2009, **42**, 135.
28 S. J. Guo, S. J. Dong and E. K. Wang, *Small*, 2009, **5**, 1869.
29 Y. Gao, C.-A. Chen, H.-M. Gau, J. A. Bailey, E. Akhadov, D. Williams and H.-L. Wang, *Chem. Mater.*, 2008, **20**, 2839.
30 S. Xing, Y. Feng, Y. Y. Tay, T. Chen, J. Xu, M. Pan, J. He, H. H. Hng, Q. Yan and H. Chen, *J. Am. Chem. Soc.*, 2010, **132**, 9537.
31 J. Huang and R. B. Kaner, *Angew. Chem.*, 2004, **116**, 5941.
32 L. Li, L. Ferng, Y. Wei, C. Yang and H.-F. Ji, *J. Colloid Interface Sci.*, 2012, **381**, 11.
33 S. Liu, J. Tian, L. Wang, Y. Luo and X. Sun, *RSC Adv.*, 2012, **2**, 411.
34 W. Wang, X. Jiang and K. Chen, *Chem. Commun.*, 2012, **48**, 7289.
35 X. Zhang and Z. Su, *Adv. Mater.*, 2012, **24**, 4574.
36 S. Wu, J. Dzubiella, J. Kaiser, M. Drechsler, X. Guo, M. Ballauff and Y. Lu, *Angew. Chem., Int. Ed.*, 2012, **51**, 2229.
37 D. M. Dotzauer, J. Dai, L. Sun and M. L. Bruening, *Nano Lett.*, 2006, **6**, 2268.
38 C. Sivakumar and K. L. Phani, *Chem. Commun.*, 2011, **47**, 3535.
39 L. Jiang and W. Zhang, *Electroanalysis*, 2009, **21**, 988.
40 Y. Zhang, J. Tian, S. Liu, L. Wang, X. Qin, W. Lu, G. Chang, Y. Luo, A. M. Asiri, A. O. Al-Youbi and X. Sun, *Analyst*, 2012, **137**, 1325.
41 Y.-l. Dong, H.-G. Zhang, Z. U. Rahman, L. Su, X.-J. Chen, J. Hu and X.-G. Chen, *Nanoscale*, 2012, **4**, 3969.
42 H. Jiang, Z. Chen, H. Cao and Y. Huang, *Analyst*, 2012, **137**, 5560.
43 H. Cui, Z.-F. Zhang, M.-J. Shi, Y. Xu and Y.-L. Wu, *Anal. Chem.*, 2005, **77**, 6402.
44 A. Henglein, *J. Phys. Chem.*, 1993, **97**, 5457.
45 Z. Zhang, A. Berg, H. Levanon, R. W. Fessenden and D. Meisel, *J. Am. Chem. Soc.*, 2003, **125**, 7959.
46 C. K. Mathews, K. E. Van Holde and K. G. Ahern, *Biochemistry*, Benjamin Cummings, San Francisco, Calif., 3rd edn, 2000.